

*Organophotocatalysis in nanostructured softgel materials*  
Supporting Information

## ***Supporting Information***

### **Organophotocatalysis in nanostructured softgel materials as tunable reaction vessels: Comparison with homogeneous and micellar solutions**

*Jürgen Bachl,<sup>a,b</sup> Andreas Hohenleutner,<sup>a</sup> Basab Bijayi Dhar,<sup>c</sup> Carlos Cativiela,<sup>b</sup>  
Uday Maitra,<sup>d</sup> Burkhard König,<sup>a</sup> and David Díaz Díaz<sup>\*a,b</sup>*

---

<sup>a</sup> *Institut für Organische Chemie, Universität Regensburg, Universitätsstr. 31, 93053 Regensburg, Germany. E-mail: David.Diaz@chemie.uni-regensburg.de; Fax: + 49 941 9434121; Tel.: + 49 941 943 4681*

<sup>b</sup> *Instituto de Síntesis Química y Catálisis Homogénea (ISQCH), CSIC-Universidad de Zaragoza, Pedro Cerbuna 12, 50009 Zaragoza, Spain. E-mail: diazdiaz@unizar.es; Tel.: + 34 976 76 3496*

<sup>c</sup> *CRcST, Chemical Engineering Division, National Chemical Laboratory, Dr. Homi Bhabha Road, 411008 Pune, India*

<sup>d</sup> *Department of Organic Chemistry, Indian Institute of Science, 560012 Bangalore, India*

† Electronic Supplementary Information (ESI) available: Synthesis and characterization of new compounds and materials, additional figures, tables and experimental details. See DOI: 10.1039/b000000x/

*Organophotocatalysis in nanostructured softgel materials*  
Supporting Information

**Contents List**

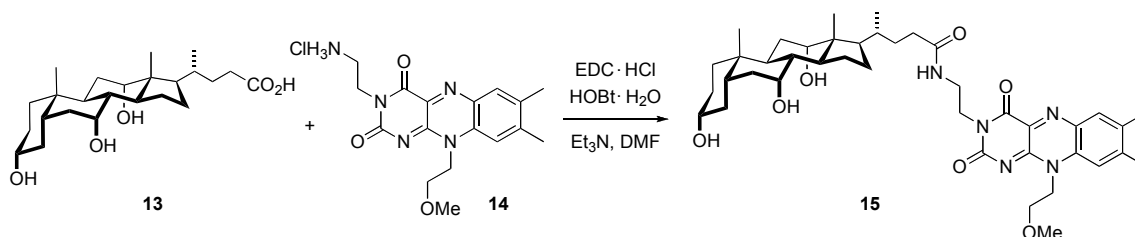
	page
1. Synthetic procedures and characterization of compounds .....	S3
2. Considerations regarding different approaches .....	S4
3. Kinetics studies .....	S6
4. Representative HPLC analyses .....	S8
5. FTIR spectroscopy .....	S8
6. UV-vis and fluorescence spectroscopy .....	S10
7. Oscillatory rheological measurements .....	S12
8. FESEM images .....	S15
9. Aeration efficiency .....	S17
10. Recycling experiments .....	S19
11. Experiments with xerogel materials .....	S19
12. Additional experiments .....	S19
13. References .....	S21

## 1. Synthetic procedures and characterization of compounds

• **General remarks:** Unless otherwise indicated,  $^1\text{H}$  and  $^{13}\text{C}$  NMR spectra were recorded at 25 °C on a Bruker Avance 600. Chemical shifts are reported in  $\delta$  (ppm) relative to the residual undeuterated solvent. Error of reported values: chemical shift 0.01 ppm ( $^1\text{H}$  NMR), 0.1 ppm ( $^{13}\text{C}$  NMR), 0.1 Hz (coupling constant  $J$ ). Melting points (m.p.) were measured with an Opti Melt Automated Melting Point System (Stanford research systems). Mass spectroscopy (ESI) was carried out on a Finnigan MAT TSO 7000. UV-vis spectroscopy was performed using a Varian Cary 50 UV spectrophotometer and quartz-glass cuvettes. Column chromatographies were performed on silica gel (70–230 or 100–200 mesh) from Merck. TLC analyses were performed on fluorescent-indicating plates (aluminum sheets precoated with silica gel 60 F<sub>254</sub>, thickness 0.2 mm, Merck), and visualization achieved by UV light ( $\lambda_{\text{max}} = 254$  nm) and staining with Liebermann-Burchard reagent. Unless otherwise indicated, solvents and reagents used in the syntheses were of p.a. grade and purchased from Sigma-Aldrich. The following gelators were also purchased from commercial suppliers and used as received without any further purification: **4** ( $\kappa$ -carrageenan; Fluka), **5** (gelatin from porcine skin, Type A; Sigma-Aldrich), **6** (*N,N'*-dibenzoyl-L-cystine; Fluka), **11** (sodium deoxycholate; Sigma-Aldrich). Polymer **3** was kindly provided by Dow Europe. **RFT**<sup>1</sup> and LMW-gelators **7**,<sup>2</sup> **8**,<sup>3</sup> **9**,<sup>4</sup> **10**<sup>5</sup> and **12**<sup>6</sup> were synthesized according to literature known procedures. Samples thus obtained exhibited identical spectroscopic data to those published. Preparation of the thermoreversible hybrid gels made of [**3** + **4**] has been also reported.<sup>7</sup> Several important reviews have been published regarding the importance of photocatalysis in organic synthesis.<sup>8</sup>

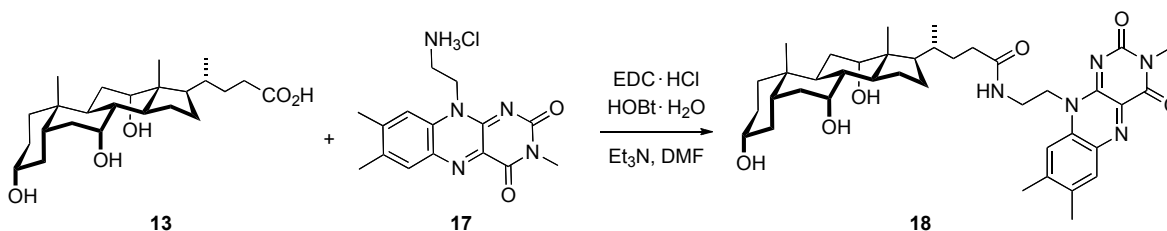
• **Synthesis and characterization of new compounds:** The following compounds were used for testing the approach II.

*N*-(2-(10-(2-Methoxyethyl)-7,8-dimethyl-2,4-dioxobenzo[*g*]pteridin-3(2*H*,4*H*,10*H*)-yl)ethyl)-4-((3*S*,5*S*,8*R*,9*R*,14*R*)-3,7,12-trihydroxy-10,13-dimethylhexadecahydro-1*H*-cyclopenta[*a*]phenanthren-17-yl)pentanamide (**15**):



To a stirred solution of compound **14**<sup>9</sup> (100 mg, 0.27 mmol) and cholic acid (**13**) (140 mg, 0.34 mmol) in dry DMF (4 mL) were added EDC·HCl (200 mg, 1.0 mmol), HOBt (100 mg, 0.74 mmol) and NEt<sub>3</sub> (0.1 mL, 0.72 mmol) at 0 °C. After 10 min, the mixture was allowed to warm to room temperature (RT) and then stirred for additional 20 h. After this time, the volatiles were evaporated under reduced pressure and the residue purified by column chromatography (eluent: EtOAc/MeOH, 10–25%) to afford compound **15** as an orange solid, which was further recrystallized from MeOH/EtOAc (140 mg, 71% yield): M.p.: decomposition at 176 °C;  $^1\text{H}$  NMR (600 MHz, CD<sub>3</sub>OD)  $\delta$  = 0.55 (s, 3H), 0.81–2.05 (m, 31 H), 2.45 (s, 3H), 2.55 (s, 3H), 3.30 (m, 3H), 3.40 (m, 1H), 3.54–3.59 (m, 2H), 3.73 (s, 1H), 3.83 (s, 1H), 3.87–3.89 (m, 2H), 4.93 (s, 3H), 7.86 (s, 1H), 7.89 (s, 1H) ppm;  $^{13}\text{C}$  NMR (150 MHz, CD<sub>3</sub>OD)  $\delta$  = 12.5, 17.7, 19.4, 21.4, 23.1, 24.2, 27.8, 28.6, 29.5, 31.1, 32.9, 34.2, 35.8 (2C), 36.5, 36.8, 38.4, 40.4, 40.9, 42.4, 42.8, 43.1, 46.2, 47.4, 48.0, 59.4, 69.0, 70.3, 72.8, 73.5, 132.3, 133.5, 136.3, 136.7, 138.6, 149.4, 150.3, 158.0, 162.2, 177.2 ppm; MS (ESI)  $m/z$  (%): 734.4 (100) [ $\text{MH}^+$ ]; UV-vis (AcOH(20%)/H<sub>2</sub>O):  $\lambda_{\text{max}}$  (log  $\epsilon$ ): 450 (3.643), 363 (3.622) nm.

4-((3*S*,5*S*,8*R*,9*R*,14*R*)-3,7,12-Trihydroxy-10,13-dimethylhexadecahydro-1*H*-cyclopenta[*a*]phenanthren-17-yl)-*N*-(2-(3,7,8-trimethyl-2,4-dioxo-3,4-dihydrobenzo[*g*]pteridin-10(2*H*)-yl)ethyl)pentanamide (**18**):



To a stirred solution of compound **17**<sup>9</sup> (45 mg, 0.13 mmol) and cholic acid (**13**) (70 mg, 0.17 mmol) in dry DMF (4 mL) were added EDC·HCl (100 mg, 0.52 mmol), HOBT (50 mg, 0.33 mmol) and NEt<sub>3</sub> (0.5 mL, 0.36 mmol) at 0 °C. After 10 min, the mixture was allowed to warm to RT and then stirred for additional 20 h. After this time, the volatiles were evaporated under reduced pressure and the residue purified by column chromatography (eluent: EtOAc/MeOH, 10–30%) to afford compound **18** (69 mg, 77% yield) as an orange solid: M.p.: decomposition at 170 °C; <sup>1</sup>H NMR (400 MHz, CDCl<sub>3</sub>) δ = 0.66 (s, 3H), 0.88 (s, 3H), 0.98 (d, *J* = 6.2 Hz, 3H), 2.40–1.01 (m, 27 H), 2.43 (s, 3H), 2.58 (s, 3H), 3.45 (m, 5H), 3.70 (m, 2H), 3.83 (s, 1H), 3.94 (s, 1H), 4.83 (t, *J* = 7.0 Hz, 2H), 7.22 (m, 1H), 7.93 (s, 1H), 8.01 (s, 1H) ppm; <sup>13</sup>C NMR (100 MHz, CD<sub>3</sub>OD) δ = 12.6, 17.7, 19.7, 21.8, 22.6, 23.4, 26.6, 27.7, 28.4, 30.6, 31.8, 32.9, 34.8, 34.9, 35.4, 35.5, 36.9, 39.6, 39.9, 41.6, 42.0, 43.7, 46.3, 46.6, 68.6, 70.6, 72.0, 73.1, 116.2, 131.4, 132.5, 135.2, 136.3, 137.3, 148.7, 148.9, 156.5, 160.2, 175.7 ppm; MS (ESI) *m/z* (%): 690.3 (100) [MH<sup>+</sup>], 1381.1 (36) [2MH<sup>+</sup>]; UV-vis (AcOH(20%)/H<sub>2</sub>O): λ<sub>max</sub> (log ε): 449 (3.648), 363 (3.619) nm.

Note: Attempts to fabricate bile acid-flavin conjugates by direct coupling **RFT** and methyl deoxycholate under Mitsunobu conditions (*i.e.*, DEAD, PPh<sub>3</sub>, THF) were fruitless. This strategy has been reported elsewhere.<sup>10</sup>

## 2. Considerations regarding different approaches

• **General remarks for all approaches:** Hydrogels were formed in double-distilled water from a Millipore filter apparatus. When necessary, dispersion of solids was achieved using a VWR™ ultrasonic cleaner (USC200TH). *Sol-to-gel* transition temperatures (*T*<sub>gel</sub>) values were determined by the “inverse flow method”: A sealed vial containing the gel was immersed upside-down in a thermostated oil bath. The temperature of the bath was raised at a rate of 2 °C min<sup>-1</sup>. *T*<sub>gel</sub> was defined herein as the temperature at which the gel was broken. In each case, the experimental error of *T*<sub>gel</sub> in at least two independent measurements was ± 2 °C. **RFT** was used instead of riboflavin due to previous studies in the group and the higher stability of the former.<sup>11</sup>

• **Approach II:** Gels were prepared according to the following procedure: Sodium deoxycholate (**11**) was weighed into a vial and a stock solution of photocatalyst **15** in MeOH was added in one portion. After slow evaporation of the MeOH, substrate **1** was added as stock solution in water and the mixture diluted with phosphate buffer (pH = 7.5) to the desired concentration (*i.e.*, 2% w/v was used as catalyst concentration for kinetics experiments). The mixture was subsequently submitted to a heating-cooling cycle to afford a stable gel within 4 h. Note that supramolecular co-assembly of **15** and **11** was necessary to induce the formation of stable gels at RT. Interestingly, this strategy afforded more stable gels in terms of thermal and mechanical properties in comparison to the gel made of only **11** (*vide infra*), suggesting a cooperative assembly of **15** and **11** during the formation of the gel network.

• **Approach III:** Bicomponent gels were prepared according to the following procedure: The mixture of **RFT** and **16** or salicylic acid (molar ratio = 1:1) was weighed into a vial and diluted with water to reach the optimized concentration (*i.e.*, 3.5 wt.% (w/v)). Note that lower amounts of **RFT** did not provide stable gels, at least in our hands. The mixture was sonicated at RT during 10 min and subsequently submitted to a heating-cooling cycle to afford the formation of stable gels at RT (Note: Herein, it is necessary to heat the mixture near 100 °C to reach the corresponding isotropic solution). In agreement with a previous report,<sup>12</sup> the formation of H-bonded complexes could be confirmed by FTIR spectroscopy (*vide infra*).

In each experiment, the vial was placed vertically above the aperture of the LED and the temperature of the mixture was held at  $20 \pm 1$  °C during the experiments via a custom made cooling apparatus as shown in Figure S1.

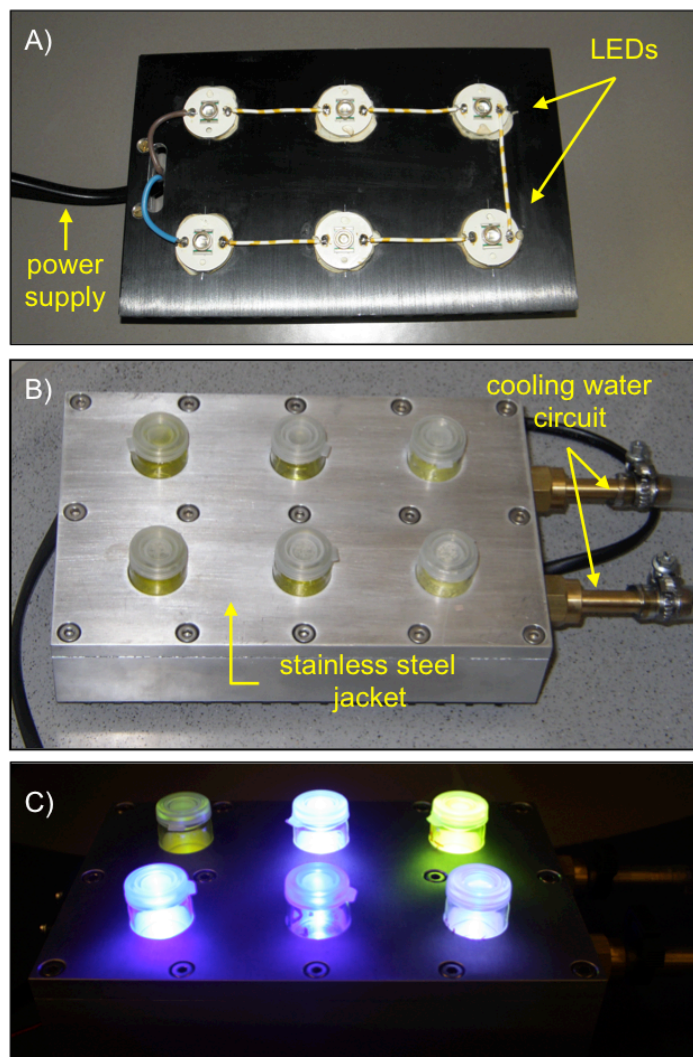


**Fig. S1** Custom made cooling apparatus with an array of six LEDs ( $\lambda_{\text{max}} = 440$  nm, 3 W) used for photooxidations: A) LEDs connected in series to a power supply. B) Set up with a stainless steel jacket to facilitate refrigeration of the vials. The distance between the LEDs and the reaction vials was adjusted to  $0.9 \pm 0.1$  cm. The apparatus allows also magnetic stirring of the mixtures. C) Typical irradiation experiment in progress.

### 3. Kinetics studies

Reaction conversions were unambiguously calculated by  $^1\text{H}$  NMR analysis of the reaction mixtures in  $\text{CDCl}_3$  according to the integration of the characteristics doublets in the aromatic region of **1** (6.81 ppm) and the oxidation product (6.87 ppm). Each experimental point represents the average of at least two randomized experiments. Among various kinetics models including zero and second order reactions, lines presented in the kinetics plots show best-fits of the first-order model for each system (Table S1, Figure S2 and Figure 6 (main paper)). However, the possibility of more complex kinetics was also suggested in some cases (*e.g.*, reactions in homogeneous and micellar solutions) where the fits were not ideal (*e.g.*, presence of an introductory phase and subsequent increase of the reaction rate to becomes first order). Thus, additional kinetics experiments at different concentrations were also performed (*vide infra*).<sup>13</sup>

As no all reactions reached full conversions, data fitting was made according to the variation of  $\ln[(\text{Ct}-\text{Cinfi})/(\text{Cinfi}-\text{C0})]$  over time, where Ct was the concentration at a given time t; Cinfi the final concentration (at infinite time) and C0 the initial concentration (at t = zero time). For reaction conversions near 100%, the plots of  $\ln(\text{Ct}/\text{C0})$  vs. time provided consistent results (Cinfi = 0). Under the above considerations, very little differences were observed between exponential and linear fit. Errors reported for the rate constants were calculated by graphical analysis.

For kinetics analyses of the reactions in gel media, the concentration of  $\text{O}_2$  available for the reaction was estimated *ca.* 950-fold higher than the substrate in a 5 mL sealed vial and 1 mL of hydrogel, and up to 30-fold if only the dissolved  $\text{O}_2$  is considered (for calculations: 1 mol (air) = 22.4 L; water solubility of  $\text{O}_2$  at 20 °C and 1 bar = 8.9 mg/L; gas constant at 20 °C = 0.0428; gas pressure = 1.013 bar; and content of  $\text{O}_2$  in air = 21%, which corresponds to 0.0091 g of  $\text{O}_2$  dissolved per Kg of  $\text{H}_2\text{O}$ ). Assuming a first order kinetics, such excess of  $\text{O}_2$  is compatible and necessary to achieve diffusion-limited rate for the reaction between  $\text{O}_2$  and the excited state of riboflavin. Increasing gelator concentration caused a modest decrease on the reaction kinetics presumably due to lower diffusion rate of reactants (*e.g.*, *ca.* 11% lower rate constant at 4-fold higher gelator concentration in the case of the gel made of gelator **4**).<sup>13</sup>

**Table S1** Expanded kinetic study of RFT-catalyzed photooxidation of **1** in homogeneous and micellar solutions at different concentrations<sup>a</sup>

solvent system <sup>b</sup>	[substrate] (mmol L <sup>-1</sup> )	[catalyst] (mol%)	[TU] (mM)	[NaDC] (mM)	irradiation time (min)	conversion (%) <sup>d</sup>	TON	TOF (min <sup>-1</sup> )	$k_{\text{obs}}$ ( $\times 10^3$ min <sup>-1</sup> )	half life, $t_{1/2}$ (min <sup>-1</sup> )
H <sub>2</sub> O/DMSO <sup>c</sup>	2.0	5.0	-	-	30	100	20.0	0.67	180.3 ± 5.66	3.8 ± 0.12
H <sub>2</sub> O/DMSO <sup>c</sup>	1.5	5.0	-	-	10	100	20.0	2.00	255.7 ± 0.21	2.7 ± 0.002
H <sub>2</sub> O/DMSO <sup>c</sup>	1.0	5.0	-	-	7	100	20.0	2.86	527.3 ± 2.83	1.3 ± 0.01
CH <sub>3</sub> CN	2.0	5.0	-	-	120	23	4.6	0.04	2.4 ± 0.07	288.8 ± 8.18
CH <sub>3</sub> CN	2.0	5.0	0.5	-	10	49	9.8	0.98	85.5 ± 2.69	8.1 ± 0.247
H <sub>2</sub> O	2.0	5.0	-	12.0	15	100	20.0	1.33	175.0 ± 7.50	4.0 ± 0.20
H <sub>2</sub> O	1.5	5.0	-	12.0	15	100	20.0	1.33	204.8 ± 7.49	3.4 ± 0.12
H <sub>2</sub> O	1.0	5.0	-	12.0	7	100	20.0	2.86	555.8 ± 21.71	1.3 ± 0.05

<sup>a</sup> Reaction conditions: T = 20 ± 1 °C; light source = blue visible light (λ = 440 nm, 3 W LED). Abbreviations: RFT = riboflavin tetraacetate; TU = thiourea; NaDC = sodium deoxycholate = **11**; TON = turnover number (catalyst productivity); TOF = turnover frequency (catalyst activity). Square brackets are used to indicate concentration. <sup>b</sup> Total solvent volume = 2 mL. <sup>c</sup> 2% (v/v) DMSO. <sup>d</sup> Reaction conversion over time for kinetics calculations was determined by  $^1\text{H}$  NMR analysis. Estimated error = ± 1.5%. Half life for first order reactions  $t_{1/2} = 0.063/k_{\text{obs}}$ .

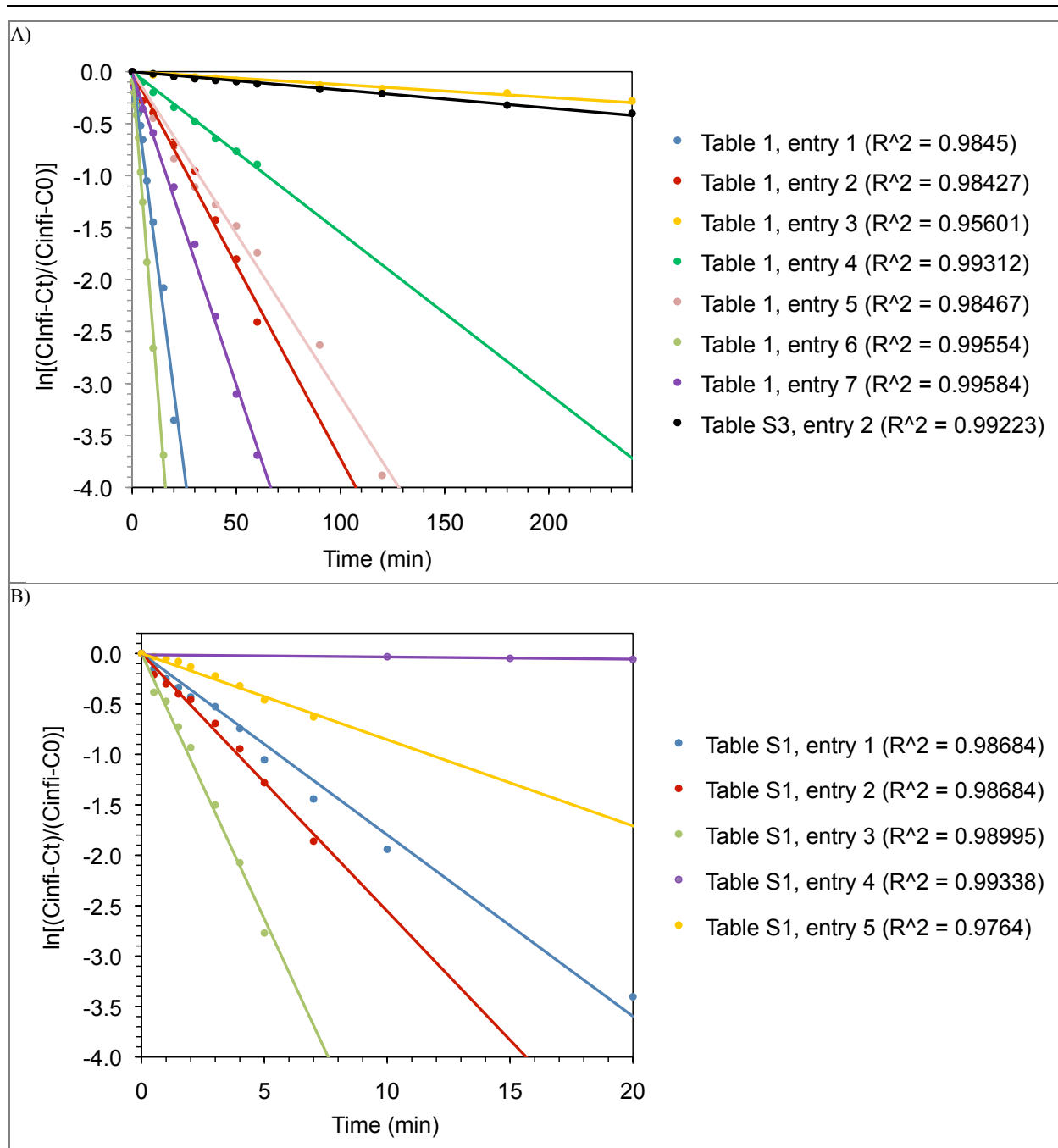


**Fig. S2** Representative best-fit first kinetics plots in homogeneous and micellar solutions according to A) Table 1 (main paper) and Table S3 (*vide infra*), and B) Table S1. Each data point represents the average of two independent measurements. Abbreviations:  $C_{infi}$  = final concentration, at infinite time;  $C_t$  = concentration at a given time  $t$ ;  $C_0$  = initial concentration, at  $t =$  zero time. Notes: a) Although the reaction in most of the cases adhere apparently well to first order behavior, some reactions such as those in  $CH_3CN$  gave similar straight lines when representing time vs. concentration or time vs.  $\ln(\text{concentration})$ , which is a signature of a reaction with substantial zero-order character. For other reactions like those in  $H_2O$ , first-order rates seems fits reasonably well until *ca.* 70% completion, after this point the reaction slows down.

#### 4. Representative HPLC analyses

High performance liquid chromatography was carried out on a HPLC 335 system (Contron Instruments) equipped with a Chiralpak AS-H, 4.6 × 250 mm, 10 μm column. In general, the reaction mixture was first extracted to separate most of the gelator. The obtained residue was further evaporated and redissolved in iPrOH (1 mL) prior injection into the HPLC column (Figure S3).

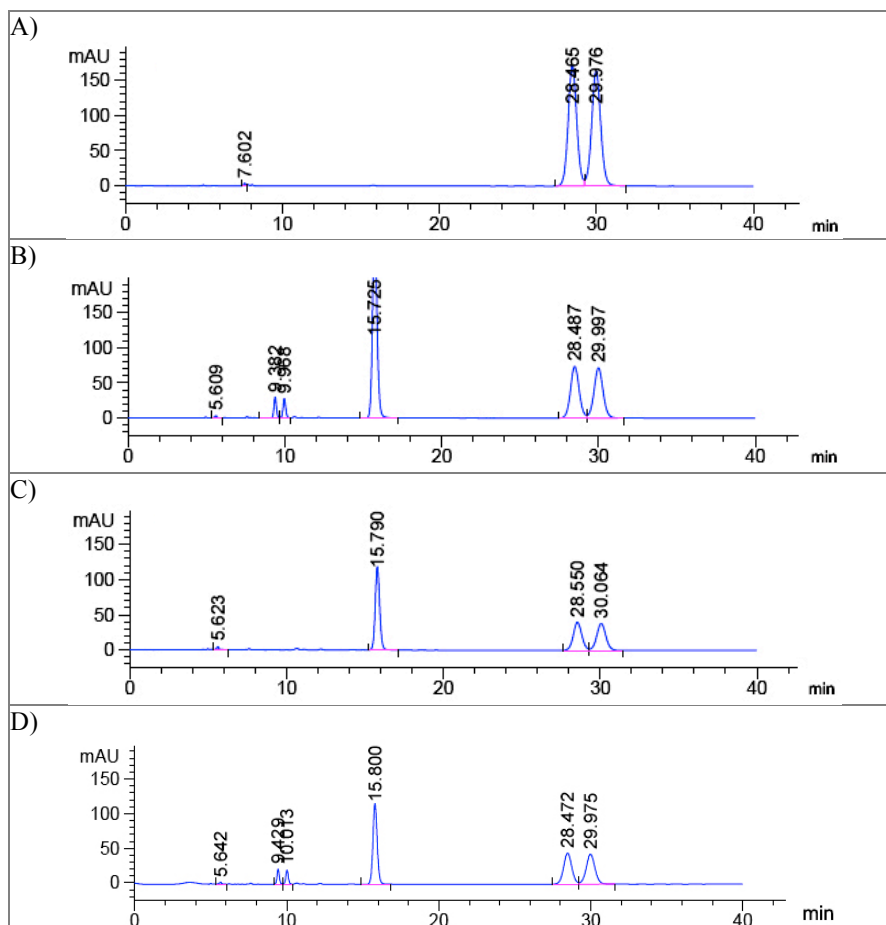
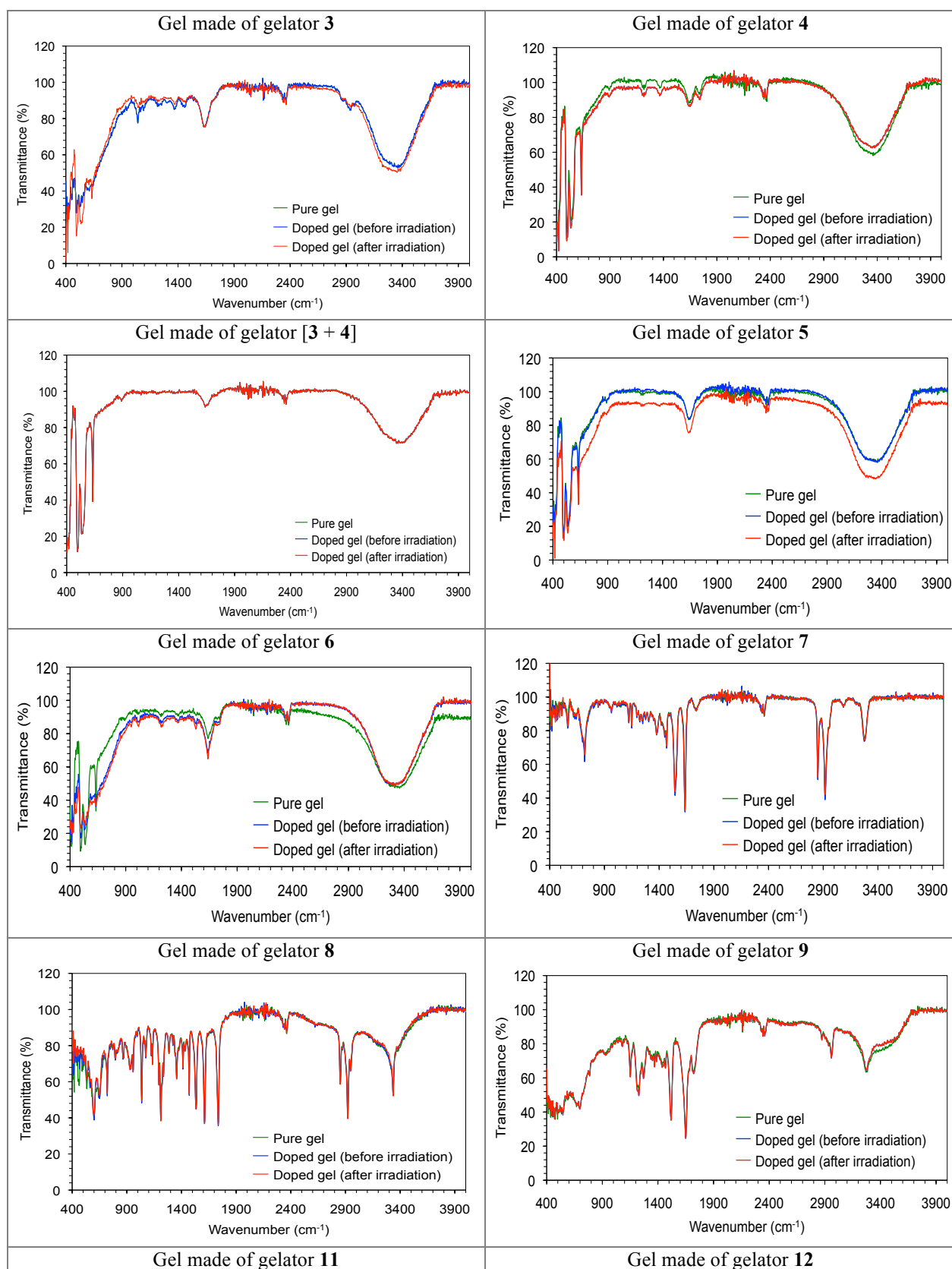


**Fig. S3** Representative HPLC traces of the products of RFT-catalyzed photooxidation of **1**. The peak at 15.7-15.8 min retention time corresponds to the reaction product (*i.e.*, 1-(4-methoxyphenyl)ethanone), whereas the reaction time for the two enantiomers of **1** are centered at 28.5 and 30 min respectively. A) HPLC trace of the racemic starting material **1**. B) Reaction using the hydrogel made of **12** (irradiation time = 20 min). C) Reaction using the hydrogel made of **11** (irradiation time = 20 min). D) Reaction carried out in micellar solution as described in Table 1 (main paper).

#### 5. FTIR spectroscopy

FT-IR spectra were recorded on a Bio-Rad Excalibur FTS 3000 MX spectrophotometer equipped with a Specac Golden Gate Diamond ATR.

In general, FTIR spectra did not show dramatic modifications of the H-bonding pattern (*e.g.*, amide I at  $\nu = 1638\text{--}1740\text{ cm}^{-1}$ , amide II at  $\nu = 1525\text{--}1635\text{ cm}^{-1}$ , H-bound OH stretching at  $\nu = 3315\text{--}3335\text{ cm}^{-1}$ ) after doping the materials (under optimized concentrations), and after irradiation (Figure S4). Alterations upon doping were more evident for bicomponent hydrogels made of [RFT + **16**] (approach III) around  $3300\text{ cm}^{-1}$ .



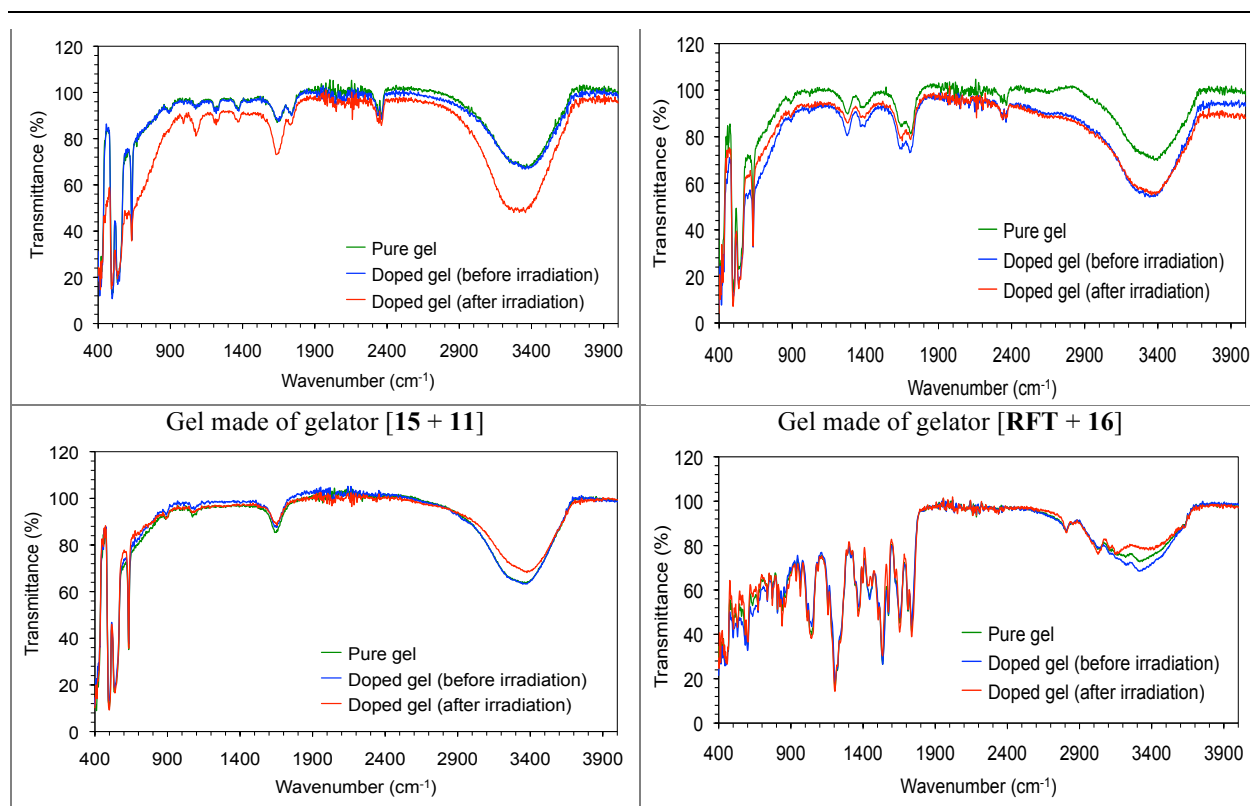


Fig. S4 Selected FTIR-spectra of non-doped and doped gels, before and after irradiation, prepared as described in the main paper.

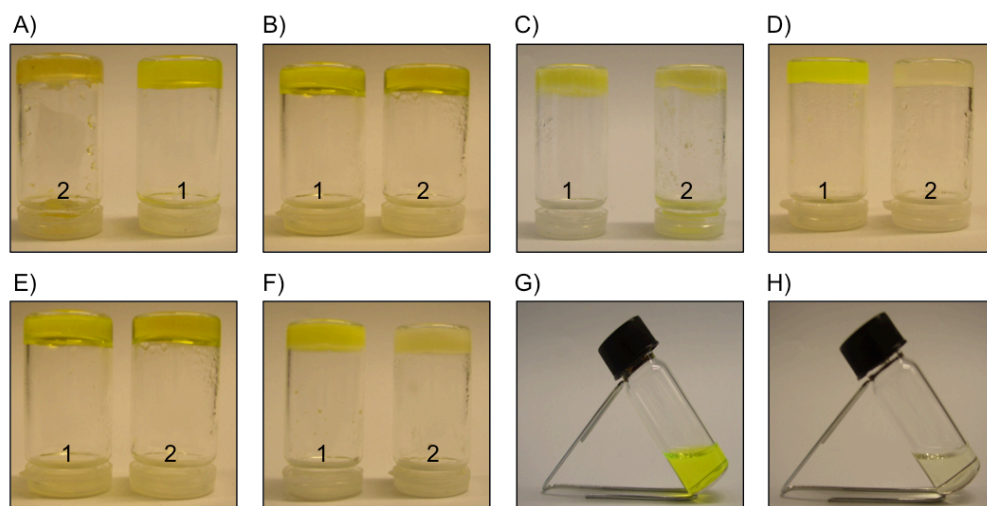
## 6. UV-vis and fluorescence spectroscopy

UV-vis spectra of translucent gel-based materials and bleaching investigation were performed using a Varian Cary 50 UV spectrophotometer and quartz-glass cuvettes of 1mm thickness. The degree of bleaching of yellowish-doped gels during the experiments was in good agreement with the decrease of the reaction rate and stagnation of the process after certain irradiation time (Table S2; Figures S5-S6).

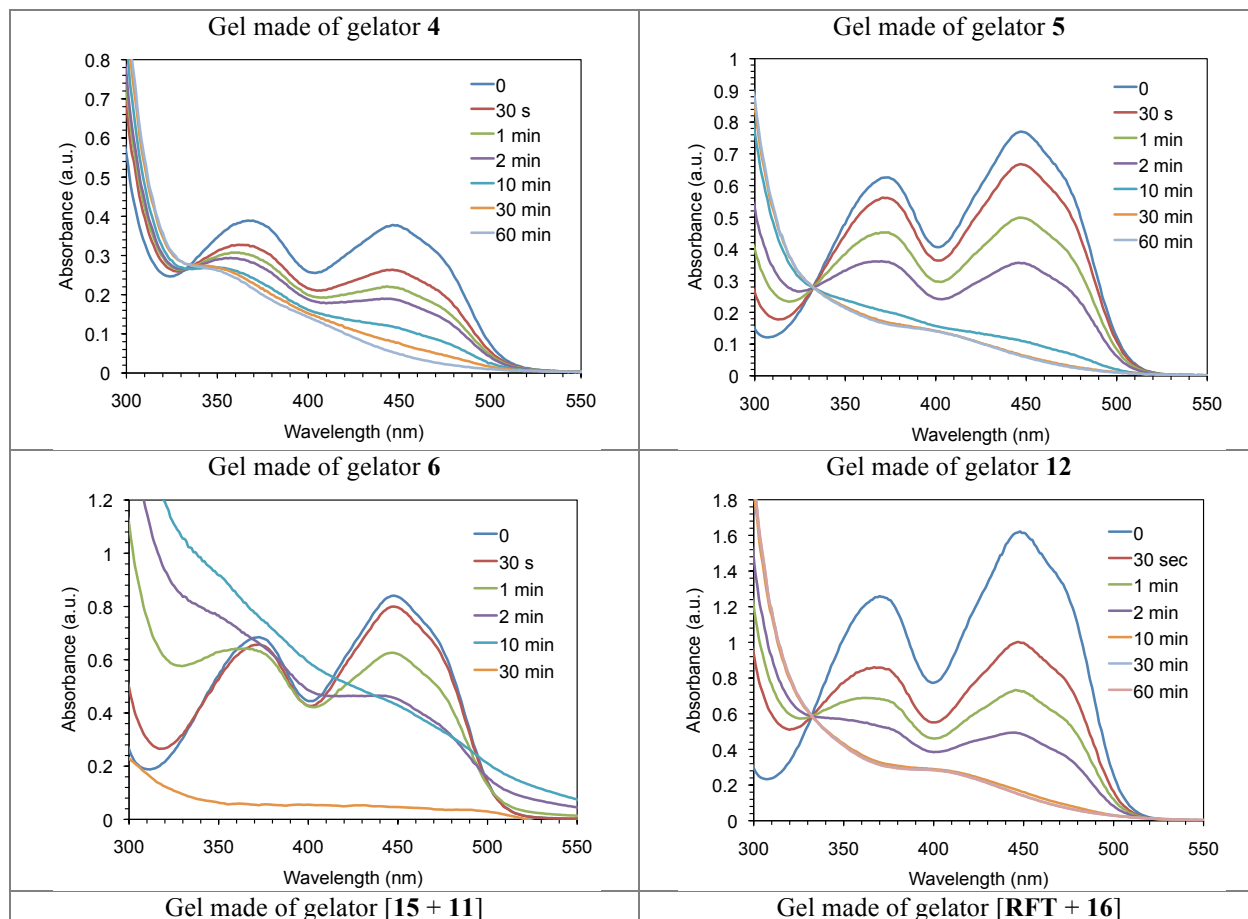
Table S2 Correlation between rate constants of RFT-catalyzed photooxidation of **1** and observed bleaching of the gel media<sup>a</sup>

entry	gelator system	solvent system	irradiation time (min)	conversion (%)	rate constant $k_{\text{obs}}$ ( $\times 10^{-3} \text{ min}^{-1}$ )	bleaching time (min)
1	<b>3</b>	H <sub>2</sub> O	120	83	$17.3 \pm 0.07$	> 4 h <sup>b</sup>
2	<b>4</b>	H <sub>2</sub> O	120	90	$20.8 \pm 0.49$	>> 4 h <sup>c</sup>
3	<b>3 + 4</b>	H <sub>2</sub> O	120	96	$28.2 \pm 2.76$	>> 4 h <sup>c</sup>
4	<b>5</b>	H <sub>2</sub> O	120	76	$12.3 \pm 0.42$	> 4 h <sup>b</sup>
5	<b>6</b>	H <sub>2</sub> O/DMSO	120	23	$2.7 \pm 0.21$	$25 \pm 5$ <sup>d</sup>
6	<b>7</b>	CH <sub>3</sub> CN	60	100	$72.6 \pm 8.34$	>> 4 h <sup>c</sup>
7	<b>8</b>	H <sub>2</sub> O	120	70	$11.0 \pm 0.07$	$50 \pm 5$
8	<b>9</b>	H <sub>2</sub> O	120	69	$11.5 \pm 0.57$	$40 \pm 5$
9	<b>10</b>	0.5 M NaCl	360	14	$0.5 \pm 0.07$	$15 \pm 5$
10	<b>11</b>	PBS	120	55	$7.3 \pm 0.07$	$40 \pm 5$
11	<b>12</b>	H <sub>2</sub> O/AcOH	120	100	$19.7 \pm 0.64$	$120 \pm 10$

<sup>a</sup> Reaction conditions as described in Table 2 (main paper). <sup>b</sup> Observed slight bleaching, but the gel remains highly fluorescent after 4 h. <sup>c</sup> No visible bleaching observed after 4 h. <sup>d</sup> The gel turned silky after 5 min irradiation. Coloration disappeared completely after 25min.



**Fig. S5** Representative pictures showing visible bleaching of doped gels upon LED blue visible light irradiation ( $\lambda_{\text{max}} = 440 \text{ nm}$ , 3 W). All gels were prepared as described in the experimental section (main paper). In each case, number 1 corresponds to the gel before irradiation and number 2 to the material after irradiation: A) Doped gel made of gelator **6**. Irradiation time 30 min. B) Doped gel made of gelator **5**. Irradiation time 30 min. C) Doped gel made of gelator **8**. Irradiation time 30 min. D) Doped gel made of gelator **7**. Irradiation time 60 min. E) Doped gel made of gelator **4**. Irradiation time 30 min. F) Doped gel made of gelator **9**. Irradiation time 30 min. G) Freshly prepared fluorescent solution of **RFT** in  $\text{CH}_3\text{CN}$  (in the absence of gelator). H) Previous solution after irradiation. Catalyst photodegradation was also observed in aqueous solutions.



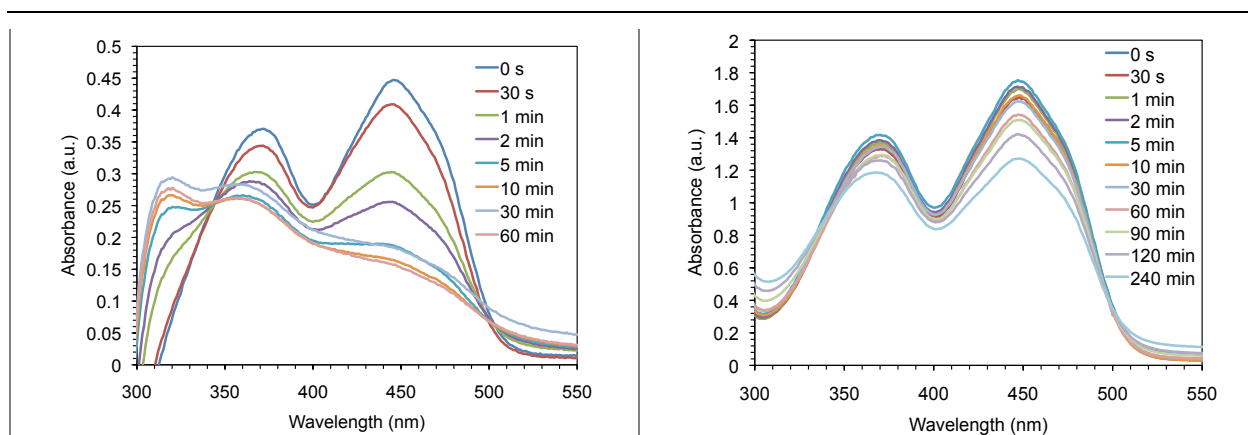


**Fig. S6** Evolution of the UV-vis spectra of various doped gels during irradiation with LED blue visible light ( $\lambda_{\text{max}} = 440 \text{ nm}$ , 3 W). Signals at  $\lambda_{\text{max}} = 373$  and 445 nm are characteristic of the **RFT** catalyst. Note that time values in the spectra do not correlate to real bleaching rates observed during kinetics experiments due to different light pathways.

To check if the environment in the gels could have any dramatic influence on the spectroscopic properties of the flavins, fluorescence spectra were also recorded on a Varian Cary eclipse spectrofluorometer. As a representative example, the absorption bands of compounds **18** and **15** at 360 and 450 nm did not show any shift upon incorporation into the gel material. The seemingly decreased absorption is due to an offset of the spectrum, probably because of light scattering effects in the gel phase (Figure 7A). In the gels, neither the wavelength nor the intensity of the emission bands was altered compared to those in the solution phase (Figure 7B). Thus, the incorporation of the compounds into the hydrogel material did not alter their spectroscopic properties, making them suitable as reaction media for photocatalysis.

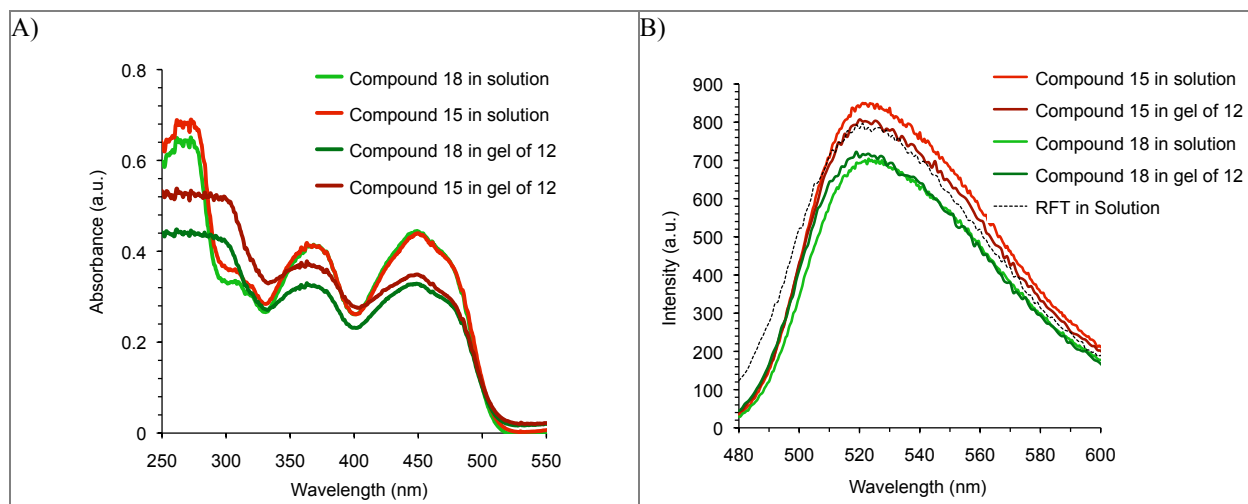


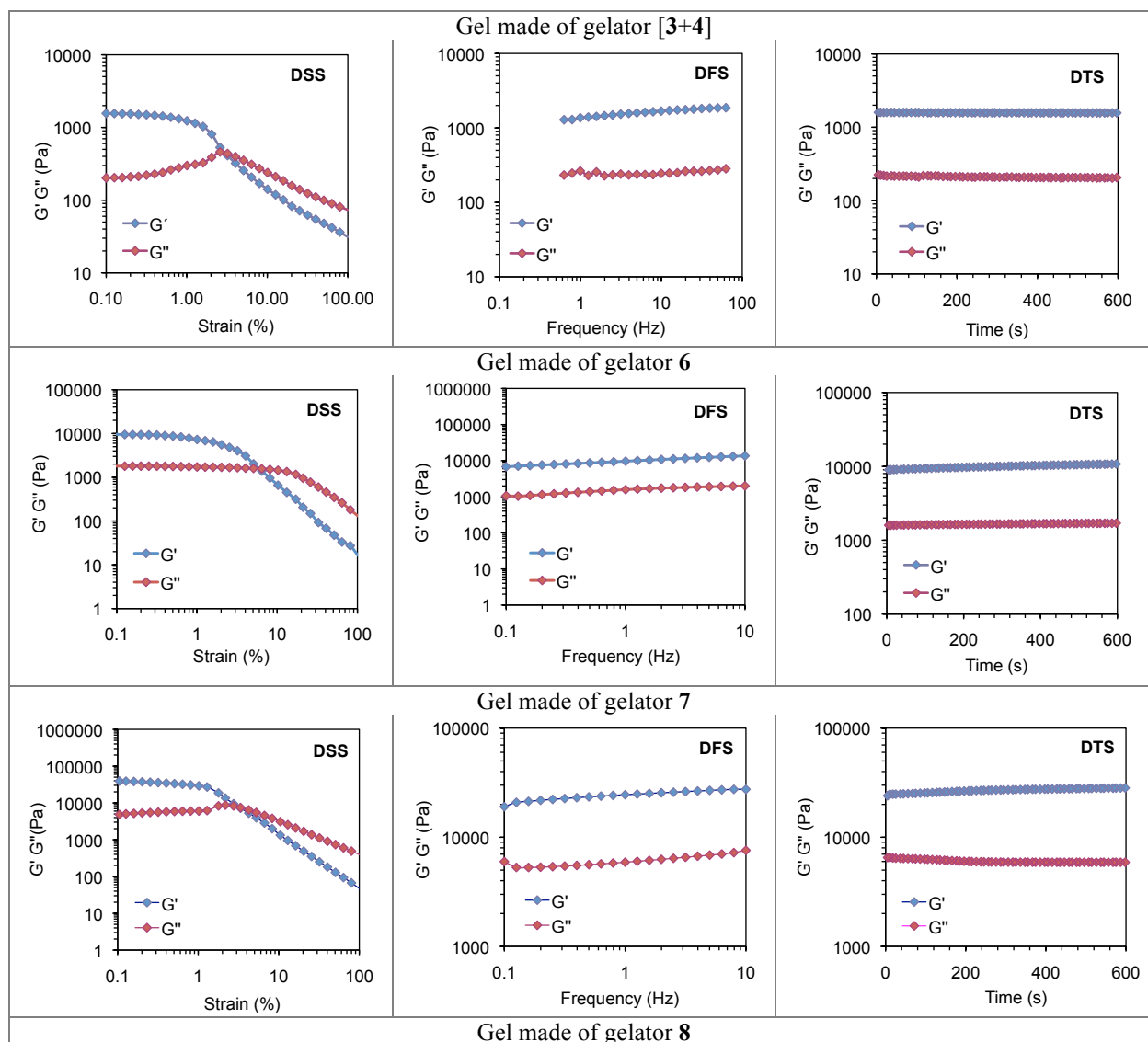
**Fig. S7** A) UV-vis spectra of compounds **18** (light/dark green) and **15** (light/dark red) in AcOH(20%)/H<sub>2</sub>O and in gels derived from gelator **12** (1%w/v in AcOH(20%)/H<sub>2</sub>O). The concentration of compounds **18** and **15** was  $1 \times 10^{-4} \text{ M}$  for all measurements. B) Representative fluorescence spectra of compounds **18** (light/dark green) and **15** (light/dark red) in AcOH(20%)/H<sub>2</sub>O and in gels derived from gelator **12** (1%w/v in AcOH(20%)/water). The concentration of compounds **18** and **15** was  $1 \times 10^{-4} \text{ M}$  for all measurements,  $\lambda_{\text{exc}} = 460 \text{ nm}$ .

## 7. Oscillatory rheological measurements

Rheological properties were determined by using an Advanced Rheometer AR 2000 from TA Instruments equipped with a Julabo C cooling system. The oscillation measurements were carried out with a 20 mm plain-plate at 25 °C.

The results were evaluated based on three type of experiments: (a) dynamic frequency sweep (DFS): Plot of  $G'$  and  $G''$  with frequency (from 0.1 to 10 Hz), performed to make sure that the frequency used in further experiments was within the linear viscoelastic regime. The results showed that the gels here are viscoelastic for frequencies ranging from 0.1 to 10 Hz; (b) dynamic strain sweep (DSS): Plot of  $G'$  and  $G''$  with strain (from 0.01 to 100%); (c) dynamic time sweep (DTS): Plot of  $G'$  and  $G''$  with time at constant strain and frequency within the viscoelastic regime. The material was defined as “gel” when  $G' > G''$  (Figure S8).

NOTE: Although manual placement of samples between the rheometer plates could sometimes provide variations in the absolute values of  $G'$  and  $G''$  between randomized measurements of the same sample, the values of  $\tan \delta (G''/G')$  were highly reproducible (differences not statistically significant,  $P > 0.5$ ).



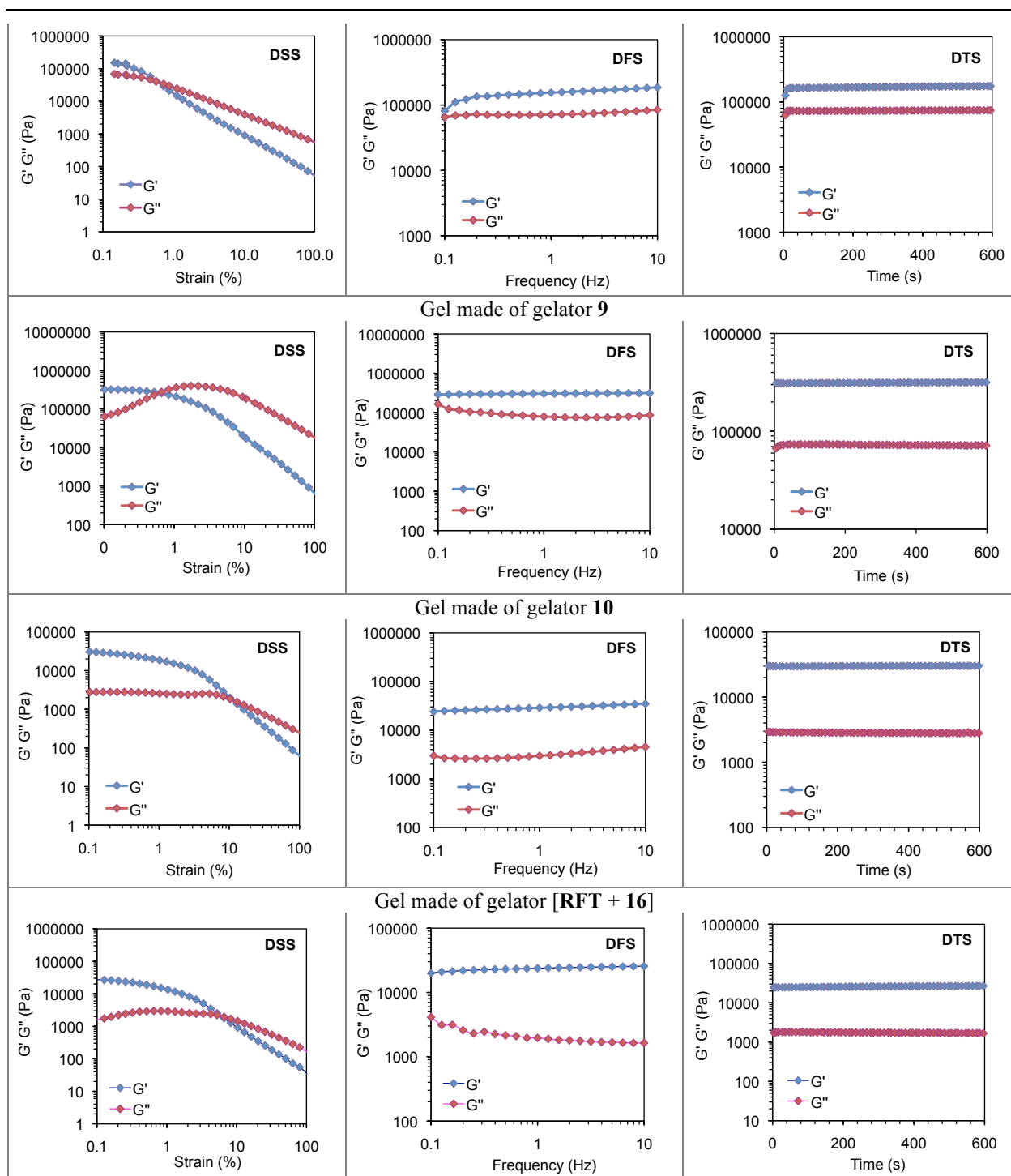


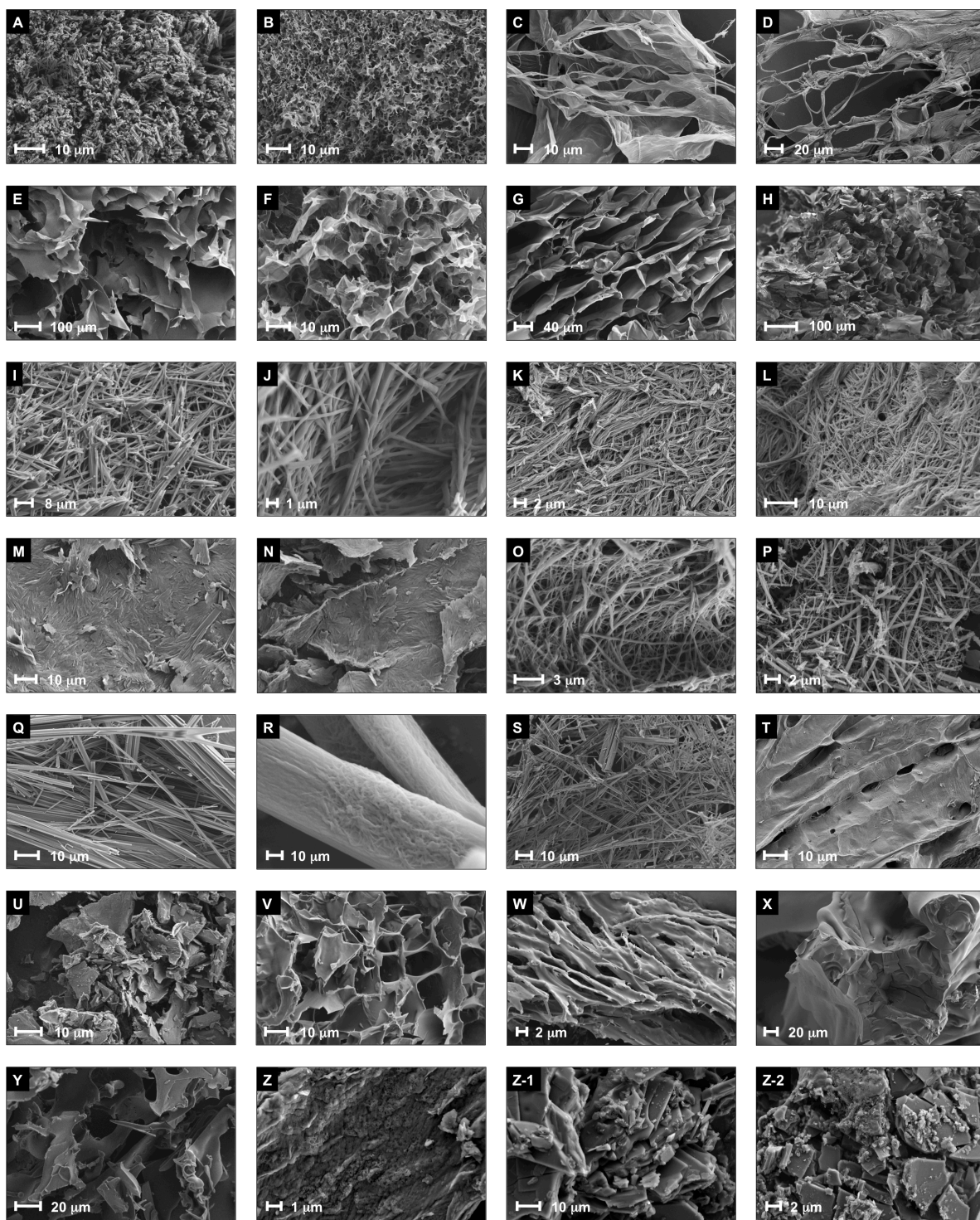
**Fig. S8** Selected oscillatory rheological plots. The results confirmed the viscoelastic nature of all systems, showing an average storage modulus ( $G'$ ) at least one order of magnitude higher than the loss modulus ( $G''$ ) within the linear regime. All gels were prepared as described in the main paper. Doping the gels with catalyst and substrate under optimized conditions caused small variations on their damping properties (e.g.,  $\tan \delta$  (pure hydrogel made of **4**) =  $0.08 \pm 0.028$ ,  $\tan \delta$  (doped hydrogel made of **4**) =  $0.07 \pm 0.013$ );  $\tan \delta$  (pure hydrogel made of **11**) =  $0.82 \pm 0.076$ ;  $\tan \delta$  (doped hydrogel made of **11**) =  $0.93 \pm 0.006$ ).

## 8. FESEM images

Specimens were observed with a Carl Zeiss Merlin field emission scanning electron microscope (FESEM, resolution 0.8 nm) equipped with a digital camera and operating at 5 kV (accelerating voltage) and 10  $\mu$ A (emission current).

Samples of the cryogels were prepared by the freeze-drying (FD) method:<sup>14</sup> An eppendorf tube (1 mL) containing the corresponding gel (100–200  $\mu$ L) was frozen in liquid nitrogen or dry ice/acetone and the sample was immediately evaporated under reduced pressure for 2 days at RT (a high vacuum pump (0.6 mmHg) or a lyophilizer were used to dry organogel or hydrogel materials respectively). A fibrous solid was obtained, which was placed on top of a tin plate and shielded by Pt (40 mA during 60 s for SEM and 30 s for FE-SEM (film thickness  $\approx$  10 nm and 5 nm respectively) (Figure S9).

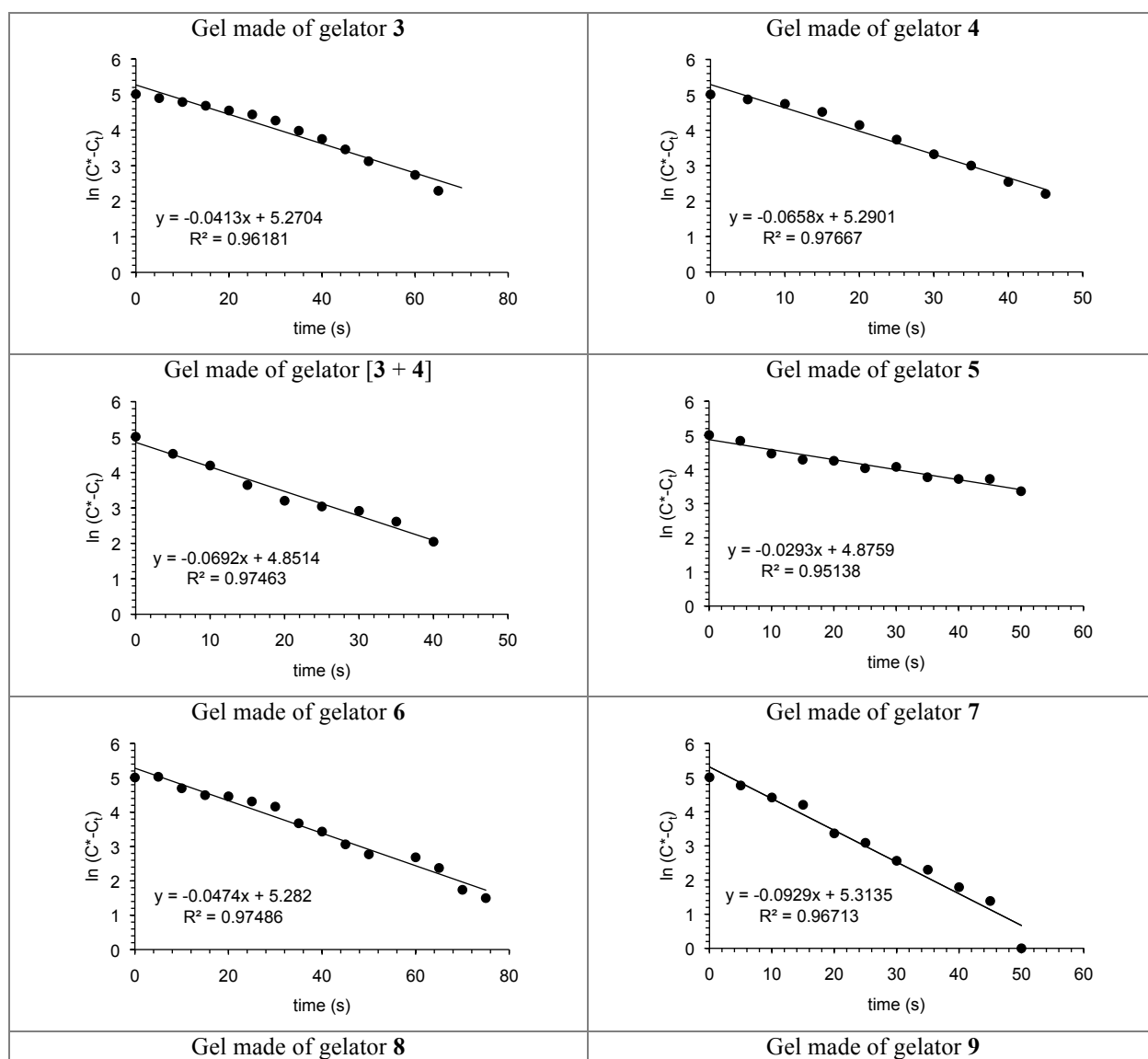
In general, shorter fibers and lower crosslinking densities were observed upon incorporation of both the substrate and the catalyst into the gel material. Such disruptive effects were minimized under the optimized conditions as described in the main paper.



**Fig. S9** FESEM images of xerogels prepared by the freeze-drying method from the corresponding pure and doped gels (*i.e.*, prepared in the absence or presence, respectively, of substrate/catalyst under optimized conditions as described in Table 2 (main paper). Abbreviations: *P* = pure; *D* = doped). Gelators are indicated next with the corresponding number in bold according to the main paper and concentrations are given in parentheses expressed as % w/v: A) *P*, **3** (5); B) *D*, **3** (5); C) *P*, **4** (2); D) *D*, **4** (2); E) *P*, [**3+4**] (2); F) *D*, [**3+4**] (2); G) *P*, **5** (1.5); H) *D*, **5** (1.5); I) *P*, **6** (0.3); J) *D*, **6** (0.3); K) *P*, **7** (0.5); L) *D*, **7** (0.5); M) *P*, **8** (3); N) *D*, **8** (3); O) *P*, **9** (3); P) *D*, **9** (3); Q) *P*, **10** (2); R) Zoom-in of image Q; S) *D*, **10** (2); T) *P*, **11** (2); U) *D*, **11** (2); V) *P*, **11** (8); W) *D*, **11** (8); X) *P*, **12** (2); Y) *D*, **12** (2); Z) *D*, [**15+11**] (2); Z-1) *P*, [**RFT + 16**] (3.5); Z-2) *D*, [**RFT + 16**] (3.5).

## 9. Aeration efficiency

Oxygen permeability of materials was measured using a DO-166MT-1 Micro Dissolved Oxygen Electrode (2 mm tip, 6 mm diameter) equipped with a data logging system (Lazar Research Laboratories, Inc.). Electrode calibration was performed at RT in air after each set of measurements (reading = 210 mV; 21% oxygen). It was critical to remove any air bubble trapped at the tip of the membrane cartridge before introducing the electrode into the gel sample. The electrode was rinsed with deionized water and dried with lab wipe after each measurement. During measurements, a constant airflow rate (0.06 bar) was maintained until saturation was reached. Relative volumetric O<sub>2</sub> transfer coefficients (volume of the gel sample was constant for all measurements = 1 mL) were obtained according to the equation  $dC_t/dt = K(C^* - C_t)$ , where  $C_t$  is the concentration of dissolved O<sub>2</sub> per unit volume at a certain time (t),  $C^*$  is the saturated dissolved O<sub>2</sub> concentration per unit volume,  $dC_t/dt$  is the change in O<sub>2</sub> concentration over a time period and  $K$  is the volumetric transfer coefficient in reciprocal time obtained from the slope of the straight tendency lines obtained by plotting  $\ln(C^* - C_t)$  vs. time (Figure S10).



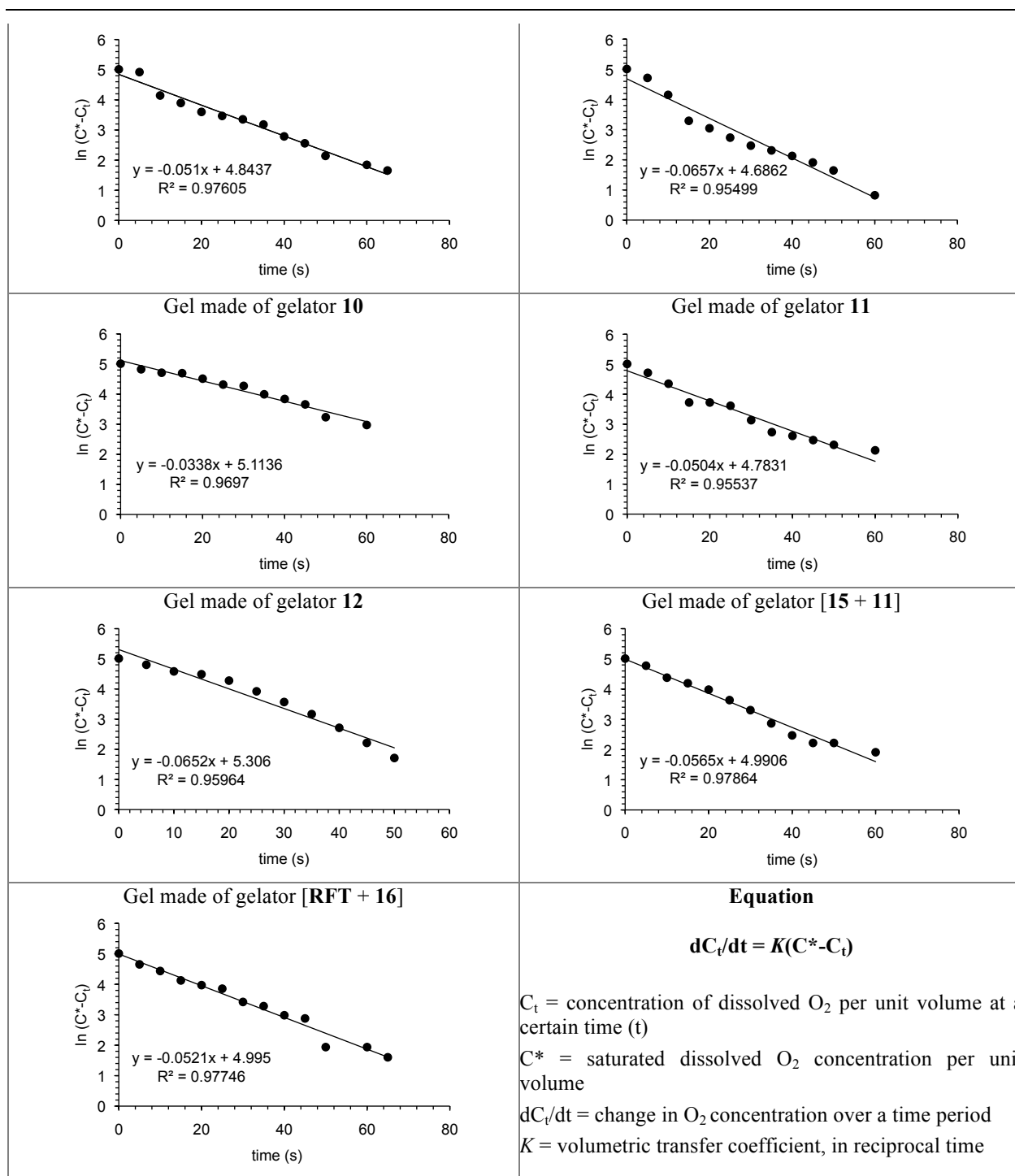


**Fig. S10** Relative aeration efficiency of the gels used as reaction vessels for RFT-catalyzed photooxidation of **1** as described in Table 2 (main paper). All plots were obtained using normalized data (the gelator used in each case is indicated). Each experimental data corresponds to the average of at least two independent measurements. Note: Although  $O_2$  determinations were quantitative; the correlation studies were essentially qualitative, as we did not quantify the individual contribution of the multiple factors that affect the aeration efficiency. No correction of temporal delays in the instrument response with respect to changes in oxygenation and perturbation of the measurements by the presence of the electrode were applied.

## 10. Recycling experiments

*General recovery procedure:* Gel materials were lyophilized after a typical irradiation-experiment (*e.g.*, 60 min, 120 min) without any previous treatment to yield the corresponding xerogels. These obtained xerogels were vigorously stirred in EtOAc (10 mL) for 30 min. The insoluble residue was filtered and washed several times with EtOAc until no yellow coloration derived from the **RFT**-catalyst could be detected (Note: UV-vis spectroscopy can be used to ensure the absence of catalyst after washing). Then, the residue was dried under vacuum and weighed. The procedure was slightly modified in the case of gelator **7** due to its moderate solubility in EtOAc: The corresponding bulk gel-material was transferred into a flask and the solvent evaporated after a typical irradiation experiment. The obtained residue obtained was crystallized from CH<sub>2</sub>Cl<sub>2</sub>/pentane (or MeOH) and washed to afford the gelator **7**, which was dried under vacuum and weighed. Thus, the recovered gelators could be used as reaction media in further experiments and recycled without any apparent detriment in their gelation ability and reaction kinetics. The weight % of recovered gelators (both LMW- and polymer-based gelators) with respect to the amount used for a particular experiment ranged between 92–98% (*e.g.*, gelator **4** = 95%; gelator **5** = 98%, gelator **7** = 92%; gelator **11** = 96%).

## 11. Experiments with xerogel materials

The use of doped photoluminescent xerogels, produced from the corresponding doped gels by the freeze-drying method, resulted inappropriate for the purposes of this work due to visible leaching of the **RFT** catalyst when swollen in aqueous or organic solutions (even under non-stirred conditions) in sufficient amounts to catalyze the photooxidation of **1**. Typically, a given gel (1 mL) doped only with **RFT** catalyst (0.0005 mM) was prepared as usual (*vide supra*). After gel formation, the material was left for 12 h at 4 °C before freezing-drying in the lyophilizer to afford the corresponding fluorescent xerogel (Figure S11). In order to test potential leaching of the catalyst, the xerogel was swelled with water (1 mL) and left in the dark without stirring for 120 min (typical reaction time). After this time, the yellowish liquid phase was removed with a syringe and evaluated for catalytic activity. Thus, an aliquot of this solution (0.2 mL) was combined with **1** (0.05 mL from a 0.1M stock solution) and the mixture irradiated (LED blue visible light,  $\lambda_{\text{max}} = 440 \text{ nm}$ ) for 60 min without stirring. The analysis of the reaction mixture revealed that the leached catalyst from the xerogel catalyzed efficiently the photooxidation of the substrate. For instance, the conversions obtained with the solutions derived from the xerogels made of gelators **4**, **5** and **11** were  $53 \pm 2.1\%$ ,  $63 \pm 1.4\%$  and  $69 \pm 1.4\%$  (error values were determined by three independent experiments).

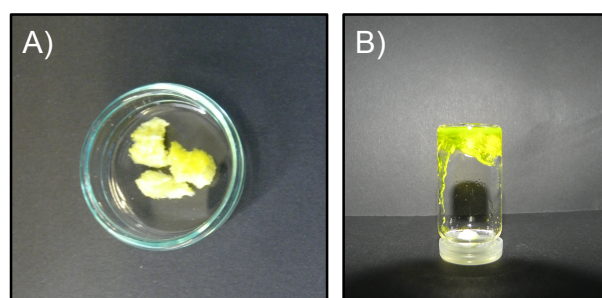


Fig. S11 A) **RFT**-containing xerogel material. B) Swelled xerogel in H<sub>2</sub>O to quantify the catalyst leaching.

## 12. Additional experiments

*12.1. Distribution of reaction product in the gel media:* Quantitative analysis of different sections of gel samples demonstrated a reasonable homogeneous distribution of the reaction product through the material. A typical experiment is given next: The gel made of gelator **3** (2% w/v) in 1 mL of water and doped with catalyst and substrate was prepared as previously described. The homogenous gel was irradiated (LED blue visible light,  $\lambda_{\text{max}} = 440 \text{ nm}$ , 3 W) at a constant temperature of 20 °C for 60 min. After this time, the bulk gel was removed from the vial and cut into 3 slices of same size (*ca.* 3 mm

thickness) using a razor blade. Thus, each slide represent a different section of the bulk cylindrical gel: bottom, middle and top sections. The samples were then diluted with brine (2 mL), melted by heating, and the homogeneous aqueous phase extracted with  $\text{CH}_2\text{Cl}_2$  ( $5 \times 5$  mL). The combined organic phases were dried over  $\text{Na}_2\text{SO}_4$ , filtered and the solvent evaporated under reduced pressure (max. 250 mbar). The obtained residues were diluted with  $\text{CDCl}_3$  (0.7 mL) and used directly for NMR analysis. The reaction conversion corresponding to each section of the gel media were calculated from two independent experiments: Top section =  $66 \pm 0.7\%$ ; middle section =  $68 \pm 1.4\%$ ; bottom section =  $71 \pm 1.4\%$ . In the experiment without slicing the bulk gel, the overall reaction conversion was established in  $68 \pm 2.5\%$ .

**12.2. Secondary amide vs. thiourea as proton transfer mediators:** The inefficiency of secondary bisamide **7** as proton transfer mediator in comparison to thiourea in  $\text{CH}_3\text{CN}$  was demonstrated with experiments performed in that solvent using **7** (0.5 mM) instead of thiourea (0.5 mM) as described in Table 1 (main paper) (Table S3). Formation of organogel with **7** was inhibited as  $0.5 \text{ mM} < \text{MGC}$ .

**Table S3** Comparison of the effect of secondary amide **7** and thiourea on the reaction rate in  $\text{CH}_3\text{CN}$  solution.<sup>a</sup>

entry	solvent <sup>b</sup>	[substrate] (mmol L <sup>-1</sup> )	[catalyst] (mol%)	[ <b>7</b> ] (mM)	[ <b>TU</b> ] (mM)	irradiation time (min)	conversion (%) <sup>c</sup>	TON	TOF (min <sup>-1</sup> )	$k_{\text{obs}}$ ( $\times 10^{-3} \text{ min}^{-1}$ )	half life, $t_{1/2}$ (min <sup>-1</sup> )
1	$\text{CH}_3\text{CN}$	5.0	10.0	-	-	240	25 <sup>d</sup>	2.5	0.01	$1.3 \pm 0.07$	$533.2 \pm 2.86$
2	$\text{CH}_3\text{CN}$	5.0	10.0	0.5	-	240	33	3.3	0.01	$1.8 \pm 0.07$	$385.1 \pm 1.50$
3	$\text{CH}_3\text{CN}$	5.0	10.0	-	0.5	120	69	6.9	0.06	$15.5 \pm 0.57$	$44.7 \pm 1.59$

<sup>a</sup> Reaction conditions:  $T = 20 \pm 1$  °C; light source = blue visible light ( $\lambda_{\text{max}} = 440$  nm, 3 W LED); vigorous stirring. Abbreviations: **TU** = thiourea; **NaDC** = sodium deoxycholate = **11**; TON = turnover number (catalyst productivity); TOF = turnover frequency (catalyst activity). Square brackets are used to indicate concentration. <sup>b</sup> Total solvent volume = 1 mL. <sup>c</sup> Reaction conversion over time for kinetics calculations was determined by <sup>1</sup>H NMR analysis. Estimated error =  $\pm 1.5\%$ . <sup>d</sup> The reaction without stirring provided only 6% conversion after 2 h.

**12.3. Approach III:** Photooxidation of **1** was fully inhibited in bicomponent hydrogels made of **RFT** and salicylic acid (*vide supra*) demonstrating the importance of the H-bonding involving the isoalloxazine moiety of **RFT** in this strategy (Figure S12).

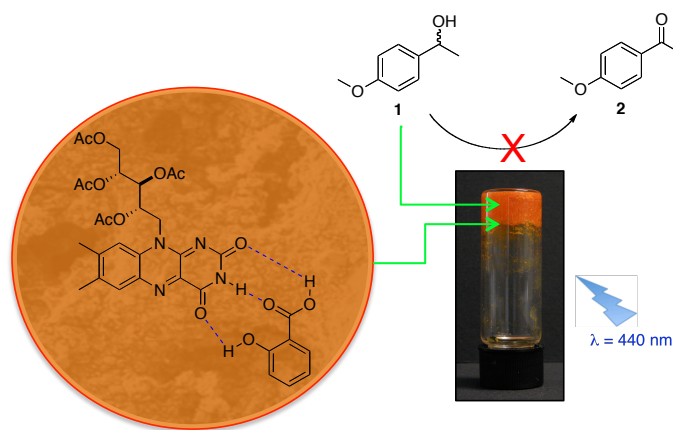


**Fig. S12** Bicomponent supramolecular hydrogel made of an equimolar mixture of **RFT** and salicylic acid (for clarity, only one possible H-bonding pattern is shown). Substrate **1** was incorporated into the gel as described in the experimental part. No conversion of **1** was observed upon irradiation apparently due to quenching of catalyst's photoluminescence (see ref. 51 in main paper).

---

### 13. References

---

- 1 A. Barthel, L. Trieschman, D. Ströhl and R. Csuk, *Arch. Pharm. Chem. Life Sci.*, 2009, **342**, 445–452.
- 2 J. H. Jung, Y. Ono and S. Shinkai, *Chem. Eur. J.*, 2000, **6**, 4552–4557; H.-J. Schanz, M. A. Linseis and D. G. Gilheany, *Tetrahedron: Asymmetry*, 2003, **14**, 2763–2769.
- 3 C. Boettcher, B. Schade and J.-H. Fuhrhop, *Langmuir*, 2001, **17**, 873–877; B. Schade, J.-H. Fuhrhop, V. Hubert, M. Weber and P. Luger, *Acta Crystallogr.*, 1997, **C53**, 1715–1717.
- 4 J. Makarevic, M. Jokic, B. Peric, V. Tomisic, B. Kojic-Prodic and M. Zinic, *Chem. Eur. J.*, 2001, **7**, 3328–3341.
- 5 S. Bhat and U. Maitra, *Tetrahedron*, 2007, **63**, 7309–7320.
- 6 S. Mukhopadhyay, H. Ira, G. Krishnamoorthy and U. Maitra, *J. Phys. Chem. B*, 2003, **107**, 2189–2192; S. Mukhopadhyay, U. Maitra, H. Ira, G. Krishnamoorthy, J. Schmidt and Y. Talmon, *J. Am. Chem. Soc.*, 2004, **126**, 15905–15914; P. Terech and U. Maitra, *J. Phys. Chem. B*, 2008, **112**, 13483–13492.
- 7 M. Tomšić, F. Prossnigg and O. Glatter, *J. Coll. Interf. Sci.*, 2008, **322**, 41–50.
- 8 See for example: G. Palmisano, V. Augugliaro, M. Pagliaro and L. Palmisano, *Chem. Commun.*, 2007, 3425–3437; J. M. R. Narayanam and C. R. J. Stephenson, *Chem. Soc. Rev.*, 2011, **40**, 102–113.
- 9 J. Svoboda, H. Schmaderer and B. König, *Chem. Eur. J.*, 2008, **14**, 1854–1865
- 10 J. K. Dutra, A. O. Cuello and V. M. Rotello, *Tetrahedron Lett.*, 1997, **38**, 4003–4004; A. P. Davis and J.-B. Joos, *Coord. Chem. Rev.*, 2003, **240**, 143–156.
- 11 C. K. Remucal and K. McNeill, *Environ. Sci. Technol.*, 2011, **45**, 5230–5237.
- 12 A. Saha, B. Roy, A. Esterrani and A. K. Nandi, *Org. Biomol. Chem.*, 2011, **9**, 770–776. Herein, we found that the use of **RFT** instead of riboflavin allowed the formation of hydrogels with higher thermal-mechanical stability, lower concentration (*i.e.*, MGC = 4% w/v for RFT and 7 % w/v for riboglavine), and without significant bleaching even after 2 h of irradiation.
- 13 Full kinetics data, individual plots, additional graphics and calculations for each experiment in this work can be obtained upon request to the authors.
- 14 S. W. Jeong and S. Shinkai, *Nanotechnology*, 1997, **8**, 179–183.